Preferred citation: H.J. Kent and M.B. Lyne. Influence of paper morphology on short term wetting and sorption phenomena. In **Fundamentals of Papermaking**, *Trans. of the IXth Fund. Res. Symp. Cambridge, 1989*, (C.F. Baker & V. Punton, eds), pp 895–920, FRC, Manchester, 2018. DOI: 10.15376/frc.1989.2.895.

INFLUENCE OF PAPER MORPHOLOGY ON SHORT TERM WETTING AND SORPTION PHENOMENA

H. J. Kent and M. B. Lyne
International Paper, Long Meadow Road, Tuxedo, NY, USA 10987

ABSTRACT

Lucas Washburn theory has been used for many years to model the penetration of liquids into paper where the rate of penetration is a function of the balance between surface tension forces and viscous drag. Interfacial contact angle is assumed to be constant and the pore morphology is reduced to an equivalent cylindrical pore radius. In reality, the pore morphology in paper is extremely complex. The interactions of liquids with paper are largely determine by local variation in Young-Laplace equilibria. Thus, the rate-determining factors for penetration of liquids in paper may be the distribution of divergence and convergence in pore wall geometry and the presence of discontinuities. In this paper, the penetration of liquids into paper coatings is examined as a function of pore morphology, pigment shape, and packing order. Sorption phenomena such as the "wetting delay" observed in uncoated but sized papers is explained in terms of the difference in morphology of surface and bulk pores. Fractal assembly rules are applied to morphological subunits in pigment coatings such that the rate of liquid penetration in a continuous coating could be predicted.

INTRODUCTION

Most of the key elements of perceived print quality are determined by the interaction of liquids with the pore system in paper. Critical aspects of this interaction are the rate and extent of mass transport from the surface of the paper. Liquid flow results in changes in the areas and/or curvature of phase boundaries and is driven by a tendency toward the establishment of hydrostatic equilibrium. Vapor phase movement tends toward establishment of diffusional or chemical equilibrium. Both equilibria and the dynamics of their establishment are functions of the curvature of liquid/vapour interfaces. The following will attempt to demonstrate ways in which the morphology of the porous medium can, by its effect on interfacial curvature, influence those equilibria and dynamics. Previous studies of the penetration of water or inks into paper have tended to use models of the pore system based on smooth, cylindrical capillaries. While it is generally acknowledged that such models are a gross simplification of the real pore geometry, they are nevertheless used because it is thought informative to be able to speak of an "effective hydrodynamic pore radius." This term is derived by applying the Lucas-Washburn equation to experimental measurements of liquid imbibition, the analogy here being with the use of "effective hydrodynamic radii" (calculated from sedimentation rates with the Navier Stokes equation) to describe the size of small irregularly shaped particles. The danger associated with such an approach is that it focuses attention exclusively on the size distribution of pores and away from factors such as shape, continuity and wall rugosity.

To explain the shortcomings of cylindrical pore models it is necessary to first digress briefly to review the basic laws of capillarity as they pertain to Young-Laplace and Kelvin equilibria.

CAPILLARITY

Young-Laplace Equilibria

The capillary system encountered in printing of coated paper consists of three phases: solid (fibre or coating), liquid (ink vehicle or water) and vapor (air, ink vehicle, water). Of particular concern are the line(s) at which these three phases meet and the shape(s) of the interface(s) between the liquid and vapor phases.

The pressure difference Δp across a liquid/vapor interface is a function of the liquid/vapor interfacial tension γ^{LV} and the mean surface curvature J of the interface, a relationship which was stated independently by Thomas Young and Pierre de Laplace in 1805:

$$\Delta p = \gamma^{LV} J \tag{1}$$

The curvature J is defined in terms of principal orthogonal radii of curvature r_1 and r_2 (1)

$$J = 1/r_1 + 1/r_2 \tag{2}$$

and many vary from point to point. The contribution of an interface to the free energy of a system is $\gamma^{LV} A^{LV}$, the product of interfacial tension and area. Minimum free energy configurations of liquid/vapour interfaces are therefore those of minimum surface area.

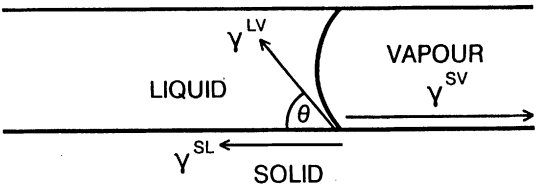

$$\gamma^{SV} = \gamma^{SL} + \gamma^{LV} \cos\theta$$

Fig. 1 Young Dupre equilibrium in a three-phase system, S solid, L liquid, V vapour

In three-phase systems (Fig. 1), this leads to an energy balance with γ^{SV} and γ^{SL}, the solid/vapor and solid/liquid interfacial tension terms:

$$\gamma^{SV} = \gamma^{SL} + \gamma^{LV} \cos \theta \qquad (3)$$

which can for simplicity be regarded as a "horizontal" resolution of forces acting at the three-phase confluence. Equation 3 is sometimes referred to as the contact angle (θ) equation or the Young-Dupre equation (2, 3) and can be regarded as a boundary condition for the Young-Laplace (4) Equation 1 in the case of a three-phase confluence located on a smooth, continuous, solid surface. The word continuous is critically important here. A pore system formed by agglomeration of fibres or pigment particles (i.e., paper or paper coating) is rich in discontinuities, both on the surfaces of individual fibres or pigment particles and at the contact points between the fibres and particles.

Contact-angle equilibrium represented by the Young-Dupre Equation 3 does not apply at a discontinuity in the solid surface. Instead a condition first described by Gibbs (5), and known as the "Gibbs inequality", is in force. The observed three-phase confluence angle ϕ can take a whole range of values depending on the geometry of the discontinuity as illustrated in Fig. 2.

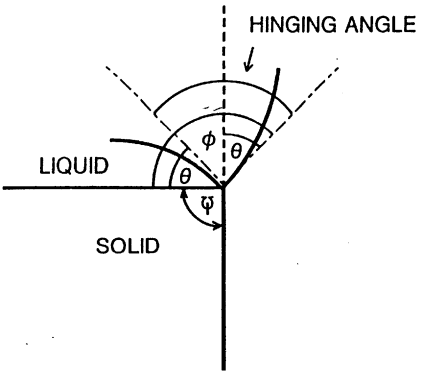

$$\phi \leq \theta + (180 - \Psi)$$

Fig. 2 Gibbs inequality hinging of a three phase confluence located at a discontinuity between two sections of solid surface S_1 and S_2

If the three-phase confluence line is considered to have been advancing along the horizontal solid surface with contact angle θ, then at the discontinuity the advance will halt as the Gibbs inequality comes into force. The "contact angle" hinges through a range of values $\phi > \theta$ until a value

$$\phi = \theta + (180 - \Psi) \tag{4}$$

is reached, Ψ being the angle of the discontinuity in Fig. 2. When condition 4 is satisfied, the angle of the three-phase confluence relative to the vertical solid surface is equal to the contact angle θ, Equation 3 comes back into force and advance of the three-phase confluence is once more possible (6).

The value of θ predicted by the Young-Dupre equation is rarely encountered in experimental measurements on real systems and this has led some workers (7, 8) to question the validity of Equation 3. It is now generally accepted that the equation is obeyed but on a microscopic scale. At the macroscopic level, the microscopic variations in chemical composition and roughness of solid surfaces lead to a phenomenon known as contact angle hysteresis (9). Here two contact angles θ_a or θ_r ($\theta_a > \theta > \theta_r$) are observed depending on whether the three-phase confluence is advancing (θ_a) or receding (θ_r) over the solid. In printing the concern will be largely with θ_a for liquids penetrating a coating, but there may well be occasions when hydrostatic pressure differences or diffusional instability cause liquid to recede from previously filled pores.

Kelvin Equilibrium

The relative vapor pressure p/p° above a liquid is dependent on the mean curvature J of the liquid/vapor interface. The relationship is expressed in simple form by the Kelvin equation (10),

$$RT \ln (p/p^\circ) = J\gamma^{LV} v^L \tag{5}$$

where v^L is the molar volume of the liquid phase, p is the vapor pressure above the curved interface and p° is the normal vapor pressure of the liquid.

Effects of vapour phase diffusion ahead of the advancing liquid front will not be dealt with here, but Equation 5 has been included to draw attention to the fact that vapour pressure is a function of interfacial curvature and as such will be

dependant on pore morphology. Everett and Haynes have provided a useful description of the interrelationship of Kelvin and Young-Laplace equilibria (11).

MATHEMATICAL MODELLING OF COATING PORES

Using the techniques of numerical integration and finite element analysis it is possible to solve the Young-Laplace equation for complex three-phase boundary configurations (12, 13). It is therefore also possible, but neither practical nor useful, to compute the exact movement of a liquid through a real pore system of arbitrary complexity. On a simpler level, similar techniques can be used to explore behavior of liquids in model pore systems.

The main features of the model presented here are:

1) two-dimensional mapping of 3D pore systems;

2) modular, morphic pore subunits based on pigment and fibre shapes; and

3) fractal subunit assembly rules.

Two-Dimensional Treatment of Capillary Phenomena in Pores

Using models of lower dimension than the real world counterpart is not new and, providing it can be done without loss of features, usually offers advantages of computational and conceptual simplicity. For example, growth and instability of two dimensional drops have been explored using perturbation analyses and have been shown to exhibit all the features of their three dimensional counterparts (14).

Placing the real three-dimensional pore structure in an (X, Y, Z) coordinate system, with X and Y parallel to the plane of the paper and the Z axis going down through the paper, the model proposed here shrinks the Y dimension to zero and deals with an (X, Z) coordinate system with X aligned in the machine direction.

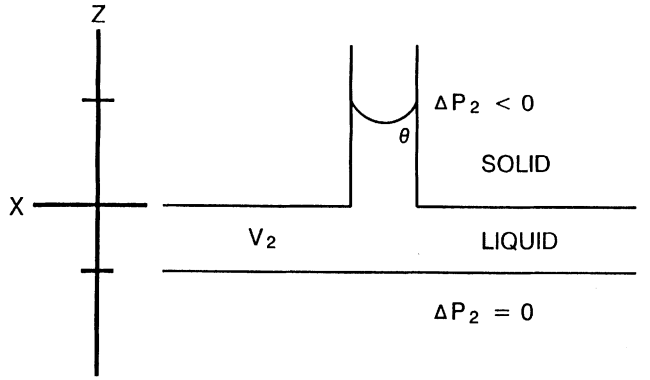

Fig. 3 (X, Z) Coordinate system for 2D model pore systems

Fig. 3 shows a representation, using the model, of a pore opening onto the surface of a paper coating which has just been printed with a layer of ink. The orientation of the diagram, with the ink layer under the coating, is intentionally the inverse of the customary representation. It permits the coating surface to be located at Z = 0 with any penetration of liquid occurring in the positive Z direction. The concepts "up" and "down" are meaningless in a coating pore system because the size of the pores is such that gravitational effects on interfacial curvature are negligible. All liquid/vapour interfaces can be safely assumed to have spherical curvature (minimum free energy configuration) and will reduce to circular arc interfaces in the model. Rather than confuse matters by speaking of liquid areas in the 2D model representing liquid volumes in the real world, a subscript 2 will be used to denote two dimensional volumes, pressures, etc. In Fig. 3 then, we have a liquid reservoir of volume V_2 outside the coating pore system (corresponding to an ink or water film) and a liquid imbibition front in the pore. The contact angle θ and the geometry of the pore wall combine to produce an interface of negative curvature J_2 resulting in a negative pressure difference ΔP_2 across the interface. The pressure on the liquid side of the interface is therefore lower than on the vapour side and also lower than at the planar liquid/vapor interface at the coating surface. Liquid from the

coating surface will flow into the pore in an attempt to establish hydrostatic equilibrium, i.e. imbibition continues until the advancing front takes on a planar configuration due to pore morphology ($\Delta P_2=0$) or the reservoir V_2 is exhausted. Provided that the morphic features of the model are chosen correctly, simulation of capillary phenomena should accurately reflect behavior in real pores.

Modular Morphic Subunits of a Pore System

Even with a two-dimensional mapping, the wide distribution of pore shapes, sizes and topographies would render an attempt to model a real pore system by detailed replication so time consuming and complex as to be of little practical value. The approach proposed here is to attempt to extract key morphic features from the components of the pore system, namely pigment particles and binders in the case of paper coatings, and to use these to design pore subunits which can then be assembled, according to some system of rules, into a complete pore system. Needless to say, the quality and realism of the final model is critically dependent on the choice of morphic subunits and their assembly rules. The following examples of morphic features extracted from clay (platey), carbonate (blocky) and synthetic (glass or plastic sphere) coatings are by no means complete and serve only as illustrations.

Platey Pigment Types

Fig. 4 shows a representation of a typical clay coating within the framework of the model.

Three morphic subunits, the Step, the Bend and the T-Junction have been extracted for the following demonstration in which the system contact angle is taken as 30°. Fig. 5 shows the progress of capillary imbibition in the Step together with the interfacial pressure-difference curve calculated from Equation 1.

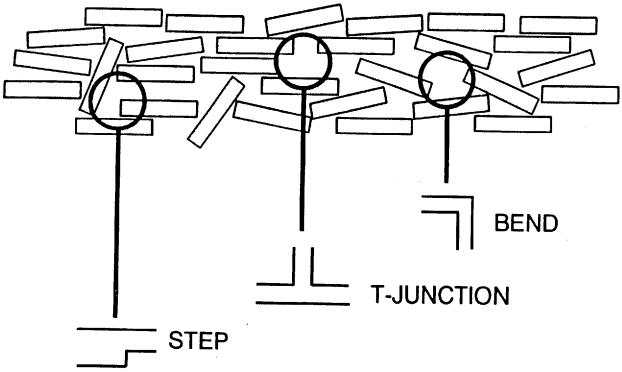

Fig. 4 Representation of a coating of platey particles showing some pore system subunits

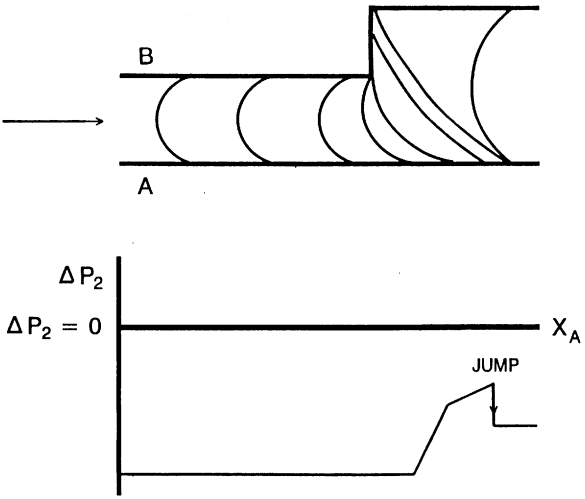

Fig. 5 The Step subunit: Interfacial configurations and pressure curve

The direction of movement of the liquid front is indicated by the arrow. In this two-dimensional model there are two distinct three-phase contact points (referred to in future as TPC's, one on each of the solid "surfaces" labeled A and B). The pressure difference curve is plotted as a function of position X_A of the A-surface three-phase confluence. The liquid initially advances driven by constant pressure (constant negative interfacial curvature) until the B TPC reaches the step discontinuity. Interfacial curvature then decreases as the A TPC continues to advance with the B TPC hinging through the Gibbs inequality. Note the associated variation in pressure. Should the pressure difference reach zero, imbibition will cease and the morphic feature can then be considered as a terminator unit in terms of the network assembly rules (see below). In this case the B TPC reaches contact-angle equilibrium before zero curvature and advance continues at constant pressure until the next discontinuity is reached at which point a non-equilibrium jump to a new stable negative imbibition pressure occurs. Had the direction of liquid advance been from the larger into the smaller pore the pressures at each end of the Step would have been the same as in the above example, but the transition between those levels would have been different. It is therefore necessary to establish the concept of capillary symmetry as an adjunct to the assembly rules for model pore systems. The Step as drawn in Fig. 5 is capillary-symmetric under rotation about the X axis, but not about the Z axis and it is therefore necessary to implement two forms of this particular subunit, the Step-up and the Step-down.

Fig. 6 shows capillary imbibition in the Bend. As in the Step, hinging of the TPC is characterized by a continuous decrease in curvature followed by a non-equilibrium jump. If both arms are of equal diameter then the Bend has complete capillary symmetry and only one form is needed. The angle of the Bend in conjunction with the contact angle determines whether or not imbibition will terminate. For the 90° bend the critical contact angle is 45°. At higher contact angles the pressure curve reaches the zero-pressure line before the moving TPC reaches the jump discontinuity.

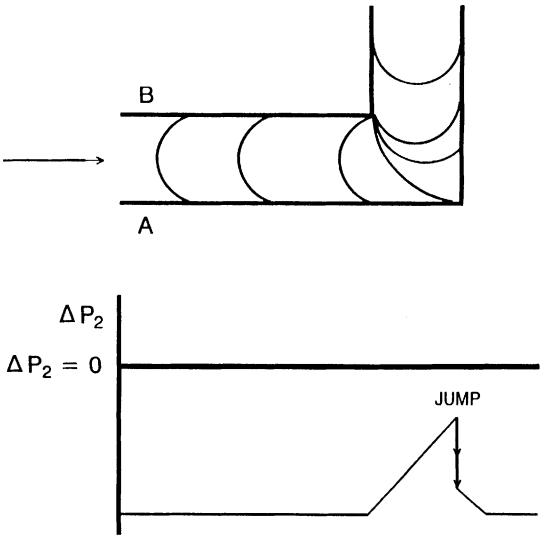

Fig. 6 The Bend subunit: Interfacial configurations and pressure curve

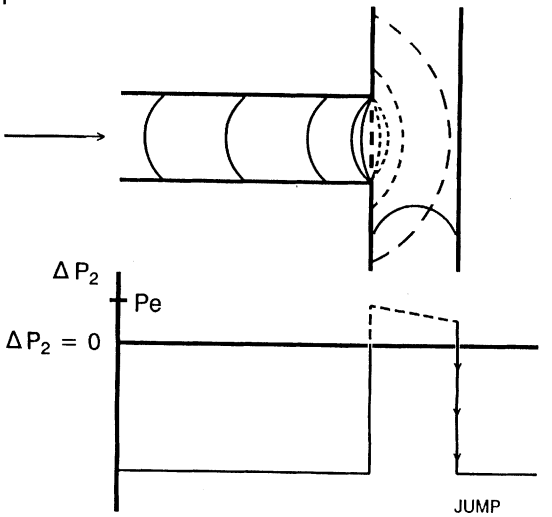

Fig. 7 The T-Junction subunit: Interfacial configurations and pressure curve

Fig. 7 shows one orientation of the capillary-asymmetric T-Junction. This type of feature might be typical of a pore at the coating surface and it is therefore interesting to note that this particular orientation is an imbibition terminator irrespective of contact angle. The advancing interface must eventually reach a planar, zero-pressure configuration from which further movement is only possible under externally applied pressure (dotted line). If that pressure is sufficient and sustained, the TPC's will re-establish contact-angle equilibrium, the interface will grow in a drop-like configuration inside the pore and will eventually contact the far wall. At that point a non-equilibrium jump back to a negative-pressure configuration occurs and further imbibition is possible. It must be stressed that this behavior is not an artifact of the two dimensional model. The same phenomena can be observed in real T-shaped cylindrical or slot pores. The external pressure needed to free the TPC's from the Gibbs inequality hinging is shown as P_e in Fig. 7 and is a function of contact angle and entrance-pore diameter (the higher the contact angle and the smaller the pore, the greater the interfacial curvature). This would suggest that with a high incidence of T-Junction pores as one might expect to find in a well ordered coating, printing pressure may be an important factor in post-printing liquid penetration.

In other orientations, with penetration occurring along one arm of the T, the T-Junction functions in a similar manner to the bend, with 45° being the critical contact angle for determining whether zero pressure is reached during hinging at the first discontinuity. For $\Theta < 45°$ the interface will eventually touch the second discontinuity, undergoing a non-equilibrium jump followed continued imbibition on two fronts.

In the examples given above, the angles formed by the discontinuities in the solid surface were all either 90° or 270°. Gibbs inequality hinging of the TPC occurred at the 90° discontinuities and non-equilibrium jumps occurred at the 270° angles. To extend a model of this type to describe factors such as the extent of order in a coating or the state of comminution of pigment particles, it is necessary to associate frequency distributions $f(\Psi_1)$, and $f(\Psi_2)$ of the discontinuity angles with the pore system subunits. As shown in Fig. 8, the distributions of hinging discontinuities Ψ_1 $(0 > \Psi_1 > 180)$ and jump discontinuity angles Ψ_2 $(180 > \Psi_2$ 360) is also dependent on pigment type (Note that the convention for angles Ψ_1 and Ψ_2 are opposite that

used in an earlier paper by the authors (15) in order to simplify measurement from within morphic features.). Examples of how such discontinuity distributions affect capillary phenomena are given below.

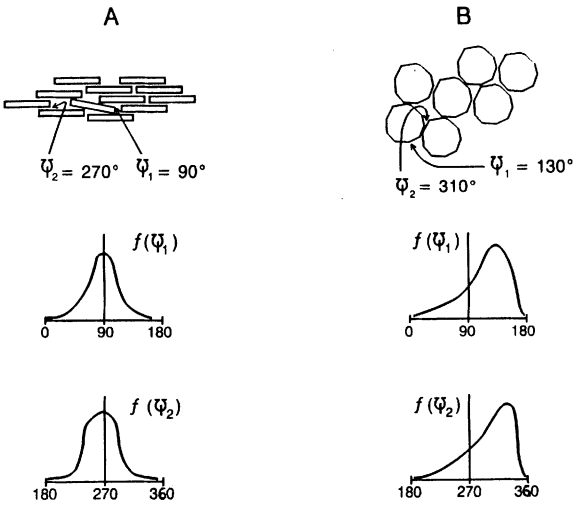

Fig. 8 Solid-surface-discontinuity frequency distributions associated with platey and blocky pigment coatings.

Blocky Pigment Types

Some morphic features of pore systems composed of blocky particles are shown in Fig. 9. Constriction I is a one-discontinuity analog of the Step and consists of connected convergent and divergent pore sections. Constriction II is the two discontinuity counterpart. The Y-Junction is similar to the T-Junction except that as shown here it is capillary symmetric. Blocky particles also give rise to large multidiscontinuity features such as the X-Junction which are less likely in platey systems.

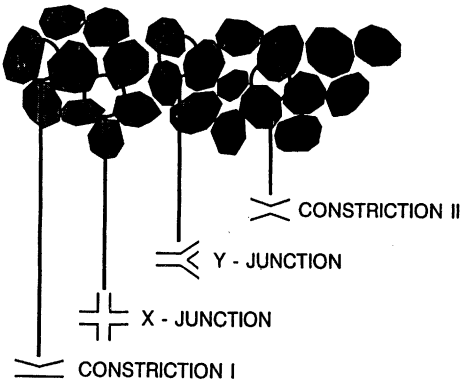

Fig. 9 Representation of a coating of blocky particles showing some pore system subunits

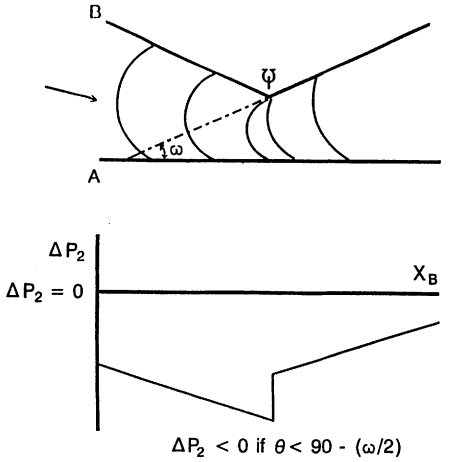

Fig. 10 The Constriction I subunit: Interfacial configurations and pressure curve

The pressure difference curve for an interface in Constriction I is shown in Fig. 10. The criterion for negative pressure throughout the hinging stage of imbibition is a function of the exit pore divergence angle ω which is in turn dependent on the discontinuity angle Ψ ($\omega = (180 - \Psi)/2$);

$$\Delta P_2 < 0 \text{ if } \Theta < 90 - (\omega/2) \qquad (6)$$

Equation 6 is the same as the criterion for capillary imbibition in a smooth divergent pore under no external pressure. Interestingly, the same criterion applies in the Y-Junction (Fig. 11) which unlike the T-Junction is not necessarily an imbibition terminator. The first part of the transition past the Ψ discontinuity can be considered as imbibition in a divergent pore of angle $\omega = 2(\Psi - 180)$. The X-Junction is somewhat more complex in that it will function as an imbibition terminator if imbibition is occurring along only one of the four arms. If imbibition occurs along two of the arms, (not necessarily simultaneously) then the condition given by Equation 6 once again determines the behavior of the penetrating liquid.

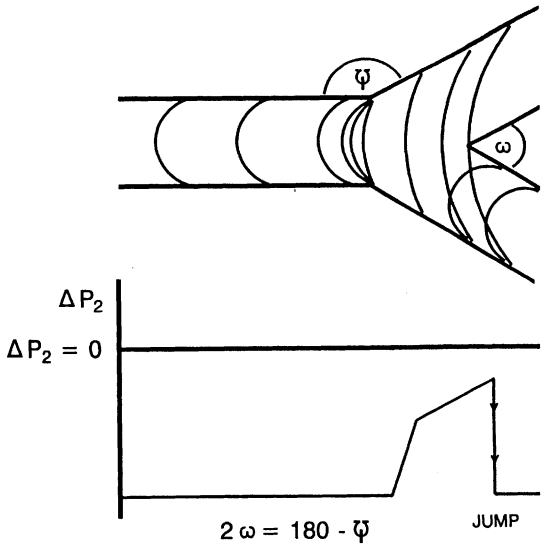

Fig. 11 The Y-Junction: Interfacial configurations and pressure curve

Spherical Particles

Pore systems in aggregates of spherical particles such as glass or plastic beads are of interest because the packing of such particles is well understood, as is the relationship between particle size and pore size. Such systems are also amenable to experimental study (16) providing a means of testing theoretical predictions of imbibition behaviour. They are, however, a somewhat specialized class of pore system in that they lack solid-surface discontinuities and can therefore not model the Gibbs inequality hinging phenomena which play such an important role in other types of paper coatings. They do, however, offer valuable insights into the roles of packing density and particle-size distribution.

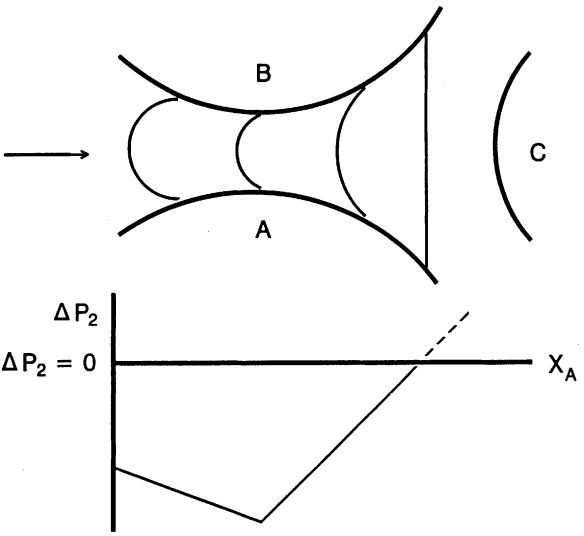

Fig. 12 The Spherical Y-Junction: Interfacial configurations and pressure curve

Fig. 12 shows a morphic subunit, analgous to the Y-Junction, formed between three spheres A, B, and C. With the sphere spacing as shown, the structure is an imbibition terminator for all possible contact angles because the curved surfaces of spheres A and B make a planar interface inevitable. If, however, the packing density is increased so that the surface of sphere C intersects the liquid interface while the curvature is still negative then a non-equilibrium jump similar to that described for the blocky-particle Y-Junction is possible and imbibition can continue. Alternatively, one could consider the effect of a fourth, smaller sphere D in the void between the three larger spheres as shown in Fig. 13. Initially the smaller sphere appears to function in a similar manner to denser packing in that it intersects the advancing interface before the pressure-difference reaches zero and thus assists further imbibition. Ultimately, however, the presence of the smaller sphere merely reconstructs a smaller version of the spherical Y-Junction and, as Fig. 13 demonstrates, eventually functions as an imbibition terminator. Of course this is not an attempt to suggest that capillary imbibition is impossible in multimodal packed-sphere pore systems. It does, however, raise the question to what extent the fraction of the pore system which is accessible to penetrating liquids may be influenced by such factors as packing density and particle size distribution.

Assembly Techniques

Having established a series of pore subunits, the next step is to try to assemble these into some sort of pore system. There are no hard and fast rules here and the assembly techniques can be tailored to suit specific needs. The following is one example based on a simple "no-branching" rule in which randomly selected subunits are linked end to end, propagating in the Z direction as shown in Fig. 14.

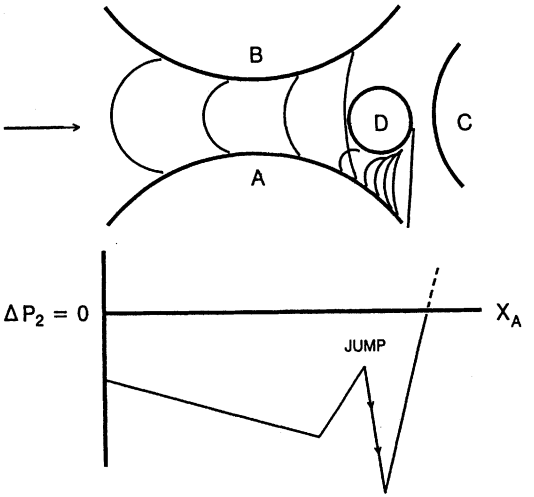

Fig. 13 Spherical Y-Junction with interstitial particle

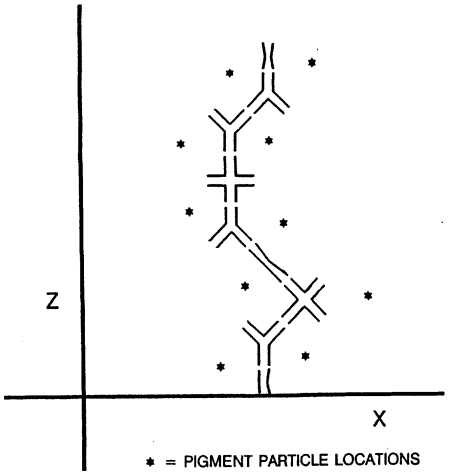

Fig. 14 "No-branching" assembly of subunits showing implied pigment particle positions

In subunits such as Y and X-Junctions with more than 2 arms, only 2 arms are connected to other subunits resulting in a single main pore with a series of short stubs attached (no branching). The implied position of pigment particles is shown in Fig. 14 and it is apparent that one can specify both the number and size of subunits such that the matrix resembles that for a particular pigment size and coating thickness. One can also specify the spatial distribution of pores to approximate realistic void volumes. The appeal of this type of modular assembly is that the capillary and hydrodynamic equations need only be solved once for each pore subunit. Having stored the pore volume and flow rate for each subunit in a computer, calculation of imbibition rates and volumes for complex multi-pore systems becomes a relatively simple matter of scaling and summation. Fractal techniques (17) are easily applied to such modular systems and allow phenomena such as binder migration and some consolidation effects to be incorporated in the model. For example, replication of a gradual reduction in pore volume towards the coating interior as a result of such processes is a simple matter of scaling such that each subsequent pore subunit is reduced in size. Varying degrees of interaction between neighbouring pores of the type in Fig. 14 could be modelled by attaching fractal branches to the unconnected subunit arms. It may in fact be possible to model a complete pore system as a single fractal curve. Space-filling trees based on Koch curves (18) can bear a remarkable similarity to the structures seen in coatings. It is tempting to speculate on the possible relationship between pore volume and the fractal dimension of such curves.

LIQUID PENETRATION INTO UNCOATED PAPER

The pores in the surface of an uncoated paper tend to be conical in shape. The basis for this approximation can be derived from network theory. Beginning with a single layer of fibres, polygons are formed by the intersection of fibres in the network. The area of each polygon hole between the fibres is proportional to the square of the average free fibre length around the hole. As further layers of fibres are added to the network the average free fibre length decreases as does the average area of the polygons. The effect of decreasing polygon area with depth is quite noticeable for the first three or four layers of fibres in paper made of softwood fibre (see Fig. 15). Similarly, Corte and Kallmes (19) have predicted that the maximum pore size in a fibre network is inversely proportional to basis weight.

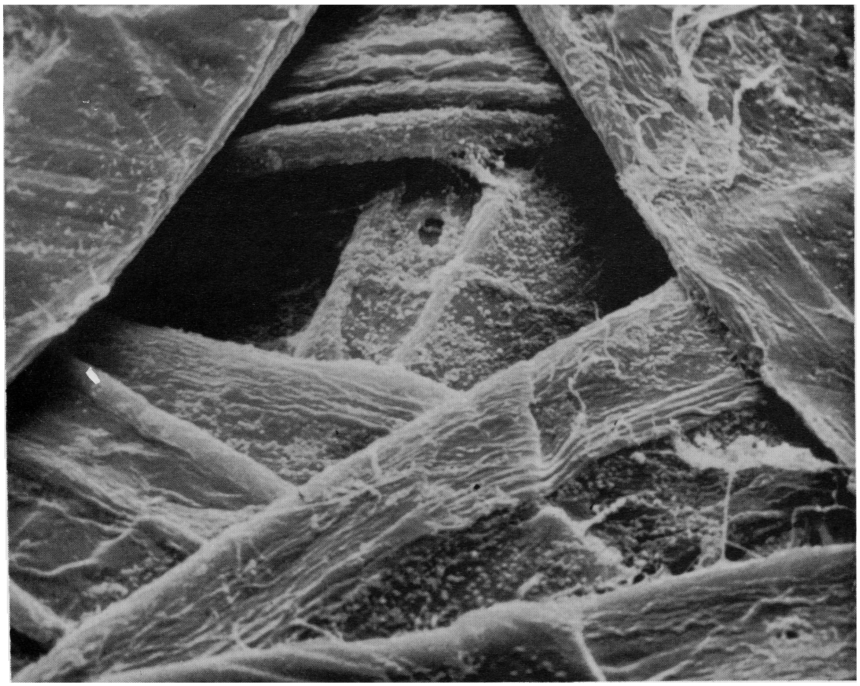

Fig. 15 Surface pore in softwood fibre network

This conical approximation is the basis for an optical instrument, the Toyoseiki Micro Topograph (20), that uses frustrated total internal reflection at four wavelengths of light to measure the average void depths of surface pores in paper. The slope of the pore walls is determined by the rate at which optical contact increases with wavelength. The intersection of the pore walls is calculated from the slope and reported as void depth. Void depths calculated by this optical instrument agree well with average roughness values determined by the Parker Print Surf air leak instrument at the same clamping pressure, and with average void depth calculated from ink transfer under corresponding printing pressure.

Thus, interstitial pores in the surface of a network of fibers are likely to be predominantly convergent. Pore wall convergence implies that liquids having contact angles slightly greater than 90 degrees will still readily penetrate and fill the surface voids in paper.

When water is introduced to the surface of sized fine paper, or self-sized newsprint, in the Bristow apparatus (21) it fills the surface voids in less that a millisecond (the minimum practicable contact time). However, water remains in the surface voids without penetrating further into these papers until an induction period usually refered to as "the wetting delay" has elapsed. While there is some debate over the exact shape of the sorption curve during this induction period (22), the rate of sorption of water is virtually nil following the initial rapid filling of the surface pores in these papers. As shown in Fig. 16 (from Ref. 21) this horizontal portion of the Bristow absorption curve is typically in the order of 100 milliseconds for water. Wetting delays for water of a similar order have been found with the Bristow apparatus by other authors (23), and by researchers using other detection techniques (24, 25).

Also shown in Fig. 16 are the sorption curves for two oils of differing viscosities. Oils do not show a penetration or wetting delay - at least not longer than the minimum contact time between the liquid and paper in the Bristow apparatus. A possible explanation for the difference in the sorption behavior of water and oil on sized papers is the tortuosity of capillaries in paper. After filling the convergent surface voids in paper the progress into divergent capillaries in the bulk of the paper of high contact angle liquids such as water is halted. Conversely, oils have a sufficiently low contact angle that a significant interfacial pressure is maintained during passage over discontinuities and through divergences in the capillary walls (see Fig. 17).

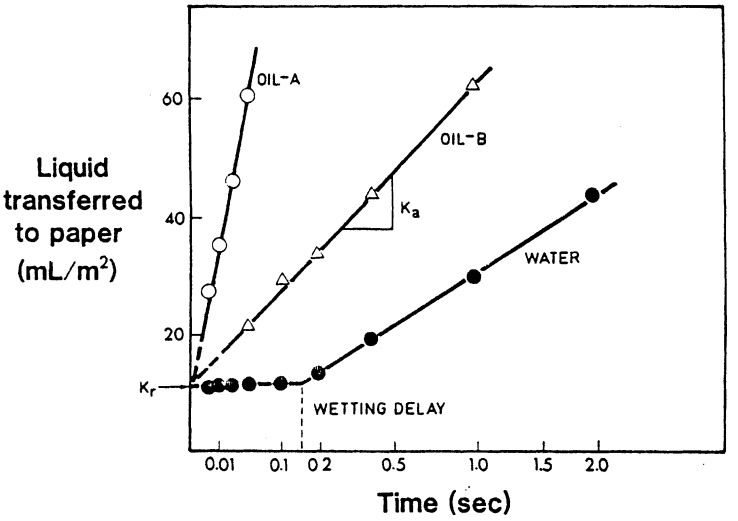

Fig. 16 Sorption curves for oils of differing viscosities and water on softwood kraft paper

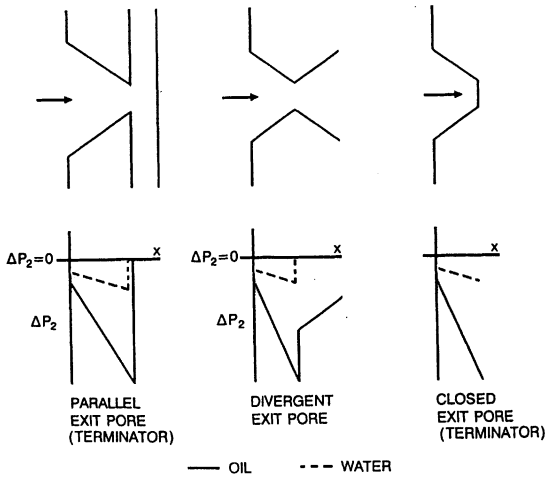

Fig. 17 Interfacial pressure curves for conical surface pores connected to various tortuous bulk pores

After the convergent surface pores are filled with water, further progress into divergent capillaries in the bulk of the paper may require the establishment of a precursor film on the capillary walls in the immediate path of the advancing water. The precursor film functions to increase the wettability of the fibre surfaces and increase interfacial curvature. This concept of changing contact angle immediately ahead of the advance of water into paper was initially proposed by Van den Akker and Wink (26). The time required for the precursor film to form would likely depend on the surface chemistry and micro roughness of the fiber surfaces (27). The rate determining factor for the penetration of water into the bulk pore structure of sized papers would then be the rate of establishment of the precursor film. For low surface free energy oils, pore morphology is more likely to be the rate determining factor. However, in both cases the retarding viscous drag forces increase with the depth of penetration of the liquid into the pore structure, so the depth of penetration remains proportional to the square root of time, as in the Lucas Washburn equation.

Another feature that distinguishes liquid uptake at the surface of paper from bulk imbibition is wicking. Wicking liquids follow grooves, or pores formed between adjacent fibres having very low convergence angles. Again, the probability of encountering this type of feature is much greater at the surface of the fibre network where fibre crossings that would interupt wicking are least frequent. The effect is easily demonstrated with a pair of hinged glass plates standing in a dish of liquid. Capillary rise in the groove between the plates increases as the angle Ψ decreases because of the effect of Ψ on the curvature of the liquid surface. As shown in Fig. 18 the capillary rise can be halted by scratching a line across the glass plates. The Ψ_1 type discontinuity thus formed can be mimicked in paper by the addition of suitable filler particles to fiber surfaces.

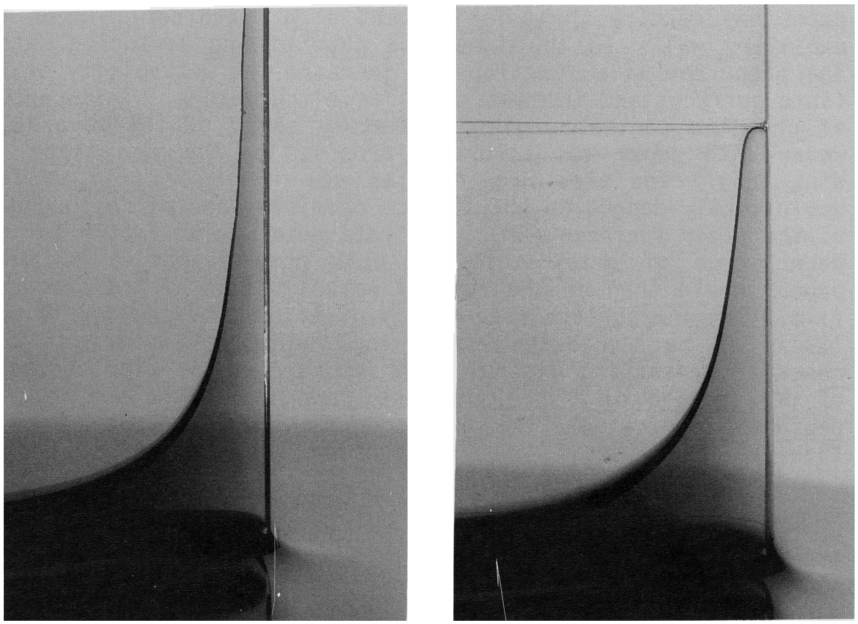

Fig. 18 Hinged glass plates in water. Note interception of capillary rise at etched line

In theory, it should be possible to modify the penetration of liquids into the bulk structure of paper in a manner similar to the effect of pigment morphology on liquid imbibition into coatings. The penetration rate of liquid into paper can be slowed dramatically by choosing fillers that create Ψ_1 type discontinuities with the fiber surfaces, or by increasing the content of a filler pigment that forms Ψ_1 type dicontinuities to the point where it virtually fills the interstitial pore structure in the fiber network.

REFERENCES

1. Adamson, A.W., Physical Chemistry of Surfaces, Second Edition, Chapter 1. New York: Interscience (1967).

2. Young, T., Phil. Trans. R. Soc, 95, 65, (1805).

3. Dupre, A., Theorie Mechanique de la Chaleur, p. 368, Paris (1869).

4. De Laplace, P.S., Mechanique Celeste, suppl. au livre X, Paris: Courcier (1806).

5. Gibbs, J.W., The Scientific Papers, Vol. 1, p. 288, New York: Dover (1961).

6. Boucher, E.A., Evans, M.J.B., and Kent, H.J., Proc. R. Soc. Lond. A 349, 81-100 (1976).

7. Jameson, G.J. and DelCerro, M.C.G., J. Chem Soc., Faraday Trans. I 72, 833 (1976).

8. Pethica, B.A., and Pethica, T.J.P., Proceedings of 2nd International Congress on Surface Activity, Vol. 3, p. 131, London: Butterworths (1957).

9. Johnson, R.E. and Dettre, R.H., Advan. Chem. 43, 112 (1964).

10. Thomson, W. (Lord Kelvin), Phil. Mag., (4) 42, 446 (1871).

11. Everett, D.H., and Haynes, J.M., Zeitschrift fur Physikalische Chemie Neue Folge, 82, 36 (1972).

12. Orr, F.M., Scriven, L.E., and Rivas, A.P., J. Coll. Interface Sci, 52, 602 (1975).

13. Boucher, E.A., Kent, H.J., Proc. R. Soc. Lond. (A356, 61 (1977).

14. Taylor, G.I., and Michaels, D.H., J. Fluid Mech., 58, 625 (1973).

15. Kent, H.J. and Lyne, M.B., "On the Penetration of Printing Ink Into Paper", Nordic Pulp and Paper, to be published, (1989).

16. Leskinen, A.M., Tappi Coating Conf. Proceedings, p. 71 (1987).

17. Mandelbrot, B.B., and VanNess, J.W., SIAM Review 10, 422 (1968).

18. Mandelbrot, B.B., Fractals: Form, Chance and Dimension, p. 69, San Francisco, W.H. Freeman (1983).

19. Corte, H. and Kallmes, O.J., The Formation and Structure of Paper, (F. Bolam, ed.) Tech. Div., B.P.B.I.F., London, p. 351, (1962).

20. Inamoto, S. and Otaka, H., Japanese Soc. of Printing Sci. & Tech. 5, 3 (1980).

21. Bristow, J.A., Svensk Papperstidning 70(19, 623 (1967).

22. Salminen, P., Studies of Water Transport in Paper During Short Contact Times, Ph.D. Thesis, Dept. Chem. Eng., Abo Akademi, Turku, Finland (1988).

23. Lyne, M.B., and Aspler, J.S., Tappi 65 (12) 98 (1982).

24. Hoyland, R.W., Howarth, P., and Field, R., Fundamental Properties of Paper Related to Its Uses, (F. Bolam, ed.), Tech. Div., B.P.B.I.F., London, p. 464 (1976).

25. Pan, Y-L., Kuga, S., and Usuda, M., Tappi, 71 (4) 119, (1988).

26. Van den Akker, J.A., and Wink, W.A., Tappi 52 (12) 2406 (1969).

27. Cazabat, A.M., and Cohen Stuart, M.A., Progress in Colloid and Polymer Science, 74, 69 (1987).

INFLUENCE OF PAPER MORPHOLOGY ON SHORT TERM WETTING AND SORPTION PHENOMENA

Dr. H. J. Kent

Dr. T.G.M. van de Ven, PAPRICAN

You have not said anything about surface heterogeneity. If one deals with surfaces of varying composition, they can give rise to exactly the same behaviour as rough surfaces i.e. sticking and jumping of contact lines without the presence of any rough edges whatsoever. Surely, in paper, this must also be a very important factor. I wonder by neglecting this, how useful your approximate approach would be?

Dr. H.J. Kent
That is a very good point. I did not actually discuss this, but we do encompass it in the model, not so much on paper fibres, but certainly in coatings. There was a slide I used (Fig. 8) which showed frequency distributions of the various types of discontinuities in both clay and carbonate coatings. With latex binder migration, you could imagine that the latex coalesces in the capillary jump type discontinuities, and you have a solid surface chemical inhomogeneity produced as the latex solidifies there. In those systems, you will replace a solid surface discontinuity with a chemical composition discontinuity exactly as you are suggesting, and these are very important in controlling capillary imbibition.

Prof. D. Eklund, Abo Akademi
Referring to the curve in Figure 16 (page 916), if you take the wetting delay and plot it on a linear scale, you will find an almost straight line. This curve has a power higher than one because of the swelling of the network in this case. If, however,

you plot it on a linear scale, you cannot observe any wetting delay or change in the linearity. Another of the references which describe a wetting delay is your Ref. 23 by Lyne and Aspler. I had the possibility to use the original values, which were sent to me by J. Aspler and plotted on a linear scale, these also fitted a straight line, with no signs of a wetting delay. This could be an appropriate place to invalidate the theory of wetting delay, which was debated at the conference 12 years ago. Further there is a comment on page 917 of your paper about the work of Van den Akker (reference 26) and the relationship between water penetration and time. To quote, "The time required for the precursor film to form would likely depend on the surface chemistry and micro roughness of the fibre surfaces ". This is the rate determining factor for the penetration of water into the bulk structure, which is linear and this linear relationship is also stated by Van den Akker.
Later on, you say, "However, in both cases, the retarding viscous drag forces increase with the depth of penetration of the liquid into the pore structures, so the depth of penetration remains proportional to the square root of time as in the Lucas Washburn equation". How can something be dependent on time and on the square root of time simultaneously?

Dr. H.J. Kent

Having listened to your presentation, I am glad I did not go into an elaborate discussion of the wetting delay in terms of capillary phenomena. I wonder whether my co-author Dr. M.B. Lyne would like to comment on this.

Dr. M.B. Lyne, International Paper Co.

With respect to Figures 16 and 17 in the paper, the pores in the surface of the paper can be modelled as truncated cones, Corte and Dodson showed this some time ago. No matter how quickly you rotate a Bristow wheel, you cannot trap the rate at which the liquid penetrates into the conical pores that constitute the surface roughness of paper. Because these pores are convergent, water fills them very rapidly and the intercept with the sorption axis is invariably positive. I think we have to rely on A. Nissan's hypothesis that the instantaneous dynamic contact angle between a fluid and a solid surface is greater than 90 degrees. So, whether there is a wetting delay or not can be debated but there is a logical explanation for the rapid penetration of the surface pores by water and the slow start to capillary penetration of bulk pores in paper.

J. Parker, BTS

Perhaps one more thing is needed to complete the story. I am glad you mentioned the open sided capillary can form in the acute crack angle between two plane surfaces. If a drop of oil is applied to a paper surface it first penetrates the paper, completely filling some of the larger capillaries. Later, however, these capillaries empty and the oil diffuses through the paper. I believe this diffusion is possible because the roughness of the fibre surfaces, together with the fibre-fibre contacts, provide a network of small capillaries through which flow can occur even if the contact angle is not quite zero.

Dr. H.J. Kent

This is a valid point and I think this is one of the reasons why it is difficult to apply this technique to fibre systems. Another difference between coatings and paper is that a pigment particle does not really change it's morphology, whereas with a fibre you can get swelling, for instance, where all those little cracks disappear as the fibre blows up so to speak.